1-1-2015

Increased phosphate transport of Arabidopsis thalianaPht1;1 by site-directed mutagenesis of tyrosine 312 may be attributed to the disruption of homomeric interactions

Elena B. Fontenot
Louisiana State University

Sandra Feuer DiTusa
Louisiana State University

Naohiro Kato
Louisiana State University

Danielle M. Olivier
Louisiana State University

Renee Dale
Louisiana State University

See next page for additional authors

Recommended Citation

Fontenot, E., DiTusa, S., Kato, N., Olivier, D., Dale, R., Lin, W., Chiou, T., Macnaughtan, M., & Smith, A. (2015). Increased phosphate transport of Arabidopsis thalianaPht1;1 by site-directed mutagenesis of tyrosine 312 may be attributed to the disruption of homomeric interactions. *Plant, Cell and Environment, 38* (10), 2012-2022. https://doi.org/10.1111/pce.12522

Plant, Cell & Environment

Plant, Cell and Environment (2015) **38**, 2012–2022 doi: 10.1111/pce.12522

Original Article

Increased phosphate transport of *Arabidopsis thaliana* Pht1;1 by site-directed mutagenesis of tyrosine 312 may be attributed to the disruption of homomeric interactions

Elena B. Fontenot[1], Sandra Feuer DiTusa[1], Naohiro Kato[1], Danielle M. Olivier[1], Renee Dale[1], Wei-Yi Lin[2], Tzyy-Jen Chiou[2], Megan A. Macnaughtan[3] & Aaron P. Smith[1]

[1]*Department of Biological Sciences and* [3]*Department of Chemistry, Louisiana State University, Baton Rouge, LA 70803, USA,* [2]*Agricultural Biotechnology Research Center, Academia Sinica, Taipei, 11529, Taiwan, China*

ABSTRACT

Members of the Pht1 family of plant phosphate (Pi) transporters play vital roles in Pi acquisition from soil and *in planta* Pi translocation to maintain optimal growth and development. The study of the specificities and biochemical properties of Pht1 transporters will contribute to improving the current understanding of plant phosphorus homeostasis and use-efficiency. In this study, we show through split *in vivo* interaction methods and *in vitro* analysis of microsomal root tissues that *Arabidopsis thaliana* Pht1;1 and Pht1;4 form homomeric and heteromeric complexes. Transient and heterologous expression of the Pht1;1 variants, Pht1;1^{Y312D}, Pht1;1^{Y312A} and Pht1;1^{Y312F}, was used to analyse the role of a putative Pi binding residue (Tyr 312) in Pht1;1 transporter oligomerization and function. The homomeric interaction among Pht1;1 proteins was disrupted by mutation of Tyr 312 to Asp, but not to Ala or Phe. In addition, the Pht1;1^{Y312D} variant conferred enhanced Pi transport when expressed in yeast cells. In contrast, mutation of Tyr 312 to Ala or Phe did not affect Pht1;1 transport kinetics. Our study demonstrates that modifications to the Pht1;1 higher-order structure affects Pi transport, suggesting that oligomerization may serve as a regulatory mechanism for modulating Pi uptake.

Key-words: *Arabidopsis*; oligomerization; phosphate transporters; transporter activity.

INTRODUCTION

All life requires phosphorus (P), a mineral nutrient crucial for energy storage, signalling, and the synthesis of nucleotides and lipids. Inorganic phosphate (Pi) is the primary form of *P* available for plant uptake, and its concentration is often low and heterogeneously distributed in soils (Raghothama 2000). As a result, agricultural systems introduce large quantities of non-renewable Pi fertilizers to increase crop yields, but the majority of the applied Pi becomes immobilized in the soil or is carried away into adjacent waterways during heavy rain events, which can lead to eutrophication. Understanding plant mechanisms of Pi acquisition and translocation may lead to the enhancement of uptake- and usage-efficiencies of Pi, which will help to ameliorate Pi deficiency, over-fertilization and resource depletion challenges.

Plant Pht1 transporters comprise a subfamily of major facilitator superfamily (MFS) transporters that catalyse proton-Pi symport (Pao *et al*. 1998; Reddy *et al*. 2012). Individual plant species have a number of Pht1 members that collectively are expressed in diverse tissues and exhibit high- and low-affinity Pi transport, functioning in Pi uptake and distribution (Schulze *et al*. 2003; Nussaume *et al*. 2011; Fan *et al*. 2013). Of the nine members of the *Arabidopsis thaliana* Pht1 family (Mudge *et al*. 2002), five have been functionally characterized: Pht1;1 and Pht1;4 are expressed at relatively high levels in the root and contribute significantly to Pi uptake (Misson *et al*. 2004; Shin *et al*. 2004; Catarecha *et al*. 2007; LeBlanc *et al*. 2013), Pht1;8 and Pht1;9 are also root-expressed and contribute to Pi acquisition (Remy *et al*. 2012), and Pht1;5 is predominantly expressed in shoots where it plays a key role in Pi distribution in accordance with Pi status and development (Nagarajan *et al*. 2011).

The mechanisms that regulate distinct Pht1 transporters are not completely understood, but a complex and multi-tiered regulatory programme is emerging. For example, transcription of *Arabidopsis* Pht1 transporters is regulated by WRKY transcription factors (e.g. WRKY45 and WRKY75), and PHR1, a MYB transcription factor recognized as a major low-Pi responsive transcriptional activator (Bari *et al*. 2006; Devaiah *et al*. 2007; Wang *et al*. 2014). In addition to transcriptional control, Pht1 transporters are regulated by a number of post-translational mechanisms, all of which are modulated by Pi availability. Proper targeting of Pht1 proteins to the plasma membrane (PM) requires PHF1, an ER localized chaperone and is influenced by a phosphorylation event (Gonzalez *et al*. 2005; Bayle *et al*. 2011). Pht1 proteins at the PM can be internalized to endosomes where they can be recycled or sent to lytic vacuoles for degradation (Bayle *et al*. 2011). Two Pi-responsive ubiquitination components, PHOSPHATE 2 (PHO2) and NITROGEN LIMITATION ADAPTATION (NLA), have been revealed to play an important role in Pht1 regulation. PHO2 is an E2 conjugase shown to target Pht1;1, and possibly other Pht1 proteins, for

Correspondence: A. P. Smith. e-mail: apsmith@lsu.edu

degradation via physical interactions within ER compartments (Huang *et al*. 2013). NLA is an E3 ligase that may act in cooperation with PHO2 to target Pht1 proteins, with an apparent preference for AtPht1;4 (Lin *et al*. 2013; Park *et al*. 2014). Notably, both *PHO2* and *NLA* transcript abundance is negatively regulated by microRNAs (miR399 and miR827, respectively), highlighting a post-transcriptional mechanism that influences Pht1 accumulation (Aung *et al*. 2006; Bari *et al*. 2006; Kant *et al*. 2011; Huang *et al*. 2013; Lin *et al*. 2013; Rojas-Triana *et al*. 2013; Liu *et al*. 2014b; Park *et al*. 2014).

Many membrane transporters can oligomerize into higher-order structures, which acts to confer structural and functional variations distinct from monomers, such as changes in affinity, catalysis and stability (Marianayagam *et al*. 2004; Clarke & Gulbis 2012; Matthews & Sunde 2012). Several membrane nutrient transporters and channels have been reported to form oligomeric structures, including *Arabidopsis* high-affinity sulphate transporters (Kataoka *et al*. 2004; Rouached *et al*. 2008), *Solanaceae* and *Arabidopsis* sucrose transporters (Reinders *et al*. 2002a,b; Schulze *et al*. 2003), ammonium transporters from tomato and *Arabidopsis* (Ludewig *et al*. 2003; Graff *et al*. 2011; Yuan *et al*. 2013), *Arabidopsis* high-affinity nitrate transporters (Okamoto *et al*. 2006; Orsel *et al*. 2006; Wirth *et al*. 2007; Sun *et al*. 2014), and *Arabidopsis* potassium channels (Obrdlik *et al*. 2004; Duby *et al*. 2008). Evidence for the oligomerization of Pi transporters stems from studies of the *Medicago truncatula* Pht1 transporter MtPT1, in which immunoblot analysis showed high molecular weight bands coinciding with possible oligomeric structures (Chiou *et al*. 2001). Additional immunoblot analysis of other Pht1 family members (Nussaume *et al*. 2011) and a dominant-negative phenotype for ectopic expression of an AtPht1;1 mutant (Catarecha *et al*. 2007) further suggests the formation of Pht1 oligomeric complexes. Recently, the crystal structure of PiPT, a Pht1 transporter from the endophytic fungus *Piriformospora indica*, shows the packing of two crystallographic threefold units that may be biologically relevant to a trimeric complex (Pedersen *et al*. 2013). However, oligomerization of Pht1 transporters has not previously been demonstrated.

Herein, we show homomeric and heteromeric oligomerization of *Arabidopsis* Pht1;1 and Pht1;4 via split *in vivo* assays and *in vitro* analysis. To better understand the underlying mechanisms involved in Pht1 oligomerization, site-directed mutagenesis was performed on a highly conserved Pi transporter motif, now recognized to play a role in Pi transporter substrate-binding (Pedersen *et al*. 2013). We show that the substitution of Tyr 312 to Asp in Pht1;1 impedes oligomerization and confers an increased Pi transport capacity in yeast. These results suggest an active site-oligomerization relationship in which oligomerization may serve as a mechanism to regulate transporter activity.

MATERIALS AND METHODS

Generation of constructs

Clones for use in SLC, mbSUS, and localization studies were generated using a PCR-based Gateway® system (Invitrogen, Carlsbad, CA, USA). Amplified *AtAMT1;1*, *AtPHT1;1*, *AtPHT1;4* and *AtPht1;1* mutant cDNAs containing appropriate attB flanking regions were cloned into pDONR™/Zeo via recombination (Invitrogen, Carlsbad, CA, USA). Constructs verified by sequencing were recombined into desired Gateway® destination vectors. Site-directed mutagenesis of *Pht1;1* was performed via overlap extension PCR as previously described (Ho *et al*. 1989). For yeast expression, *ScPHO84*, *AtPht1;1* and *AtPht1;1* mutant cDNAs were cloned into the pYES2 vector, which contains a Gal1-inducible promoter, via restriction enzyme/ligation and the resulting plasmids were sequenced for verification. Primer sequences are listed in Supporting Information Table S1.

Split luciferase complementation (SLC) assays

A. thaliana (Col-0) protoplasts were prepared and transformed as described (Kato & Jones 2010). Briefly, 1.2×10^4 protoplasts were transformed with the appropriate pDuExAc6 and pDuExDc6 vectors (2.0 μg each) in a well of a 96-well plate. These vectors constitutively express a protein of interest at the C-terminal end with NLuc- and CLuc- tags, respectively. Four independent transformations were conducted for each protein pair of interest in one experiment. The experiment was then repeated at least three times using protoplasts prepared from different plants. Relative luminescence units (RLU) were measured 16 h after transformation. RLU in the experimental and biological replicates were used to obtain means and SEs for each protein pair.

Immunoprecipitation and immunoblot analysis

Root microsomal proteins were extracted, immunoprecipitated and immunoblotted as previously described (Huang *et al*. 2013) with Pht1;1/2/3- or Pht1;4-specific antibodies.

Mating-based split ubiquitin and split-ubiquitin yeast-two-hybrid systems

Clones were transformed into yeast haploid strains THY.AP4 (*MATa;* ade2-, his3-, leu2, trp1-, ura3-; lexA::ADE2, lexA::HIS3, lexA::lacZ) and THY.AP5 (*Matα*; ade2-,his3-, leu2-, trp1-) via LiAc transformation as described (Grefen *et al*. 2009). CUb fusion isolates were tested for background activity using the lacZ reporter gene prior to mating as described (Grefen *et al*. 2009). CUb and NUb isolates were grown overnight in SC_l and SC_{tu} liquid media, respectively, at 30 °C in an orbital shaker. One millilitre of overnight culture was spun at room temperature for 5 min at 2500 g. Cells were resuspended in 200 mL yeast extract, peptone, dextrose (YPD). 15 μL of bait and prey were mixed and 10 μL of matings were plated on YPD and incubated for 10–16 h at 28 °C. Portions of matings were streaked onto SC_{tlu} plates and grown 2–3 d at 28 °C. Matings were inoculated in SC_{tlu} liquid media and incubated overnight. Cultures were diluted to OD_{600} 0.1 and grown to OD_{600}

~0.6–1.0. Cultures were diluted to OD_{600} 0.1 with water, plated onto SC_{tlum}, SC_{ahtlum}, and SC_{ahtlum} + 10 mM 3-AT and grown 3–9 d at 28 °C. Split-ubiquitin yeast two-hybrid analysis of AtPht1;1 and AtPht1;4 was performed using the DUAL membrane Kit (Dual Systems Biotech, Zurich, Switzerland) according to the manufacturer's instructions. β-galactosidase activity was observed using a chloroform overlay assay (Duttweiler 1996; Lin *et al*. 2013).

Yeast complementation assays and RNA extraction

Sequenced clones were transformed into the *Saccharomyces cerevisiae* yeast strain PAM2 (Δpho89::*TRP1* Δpho84::*HIS3 ade2 leu2 his3 trp1 ura3*) as described (Geitz *et al*. 1995; Daram *et al*. 1999). Preparation of cells for growth rate assays was adapted from Muchhal *et al*. (1996). Isolates were grown in Pi-replete (7.34 mM) SC_u media (pH 5.6) containing 2.0% sucrose until OD_{600} 0.3–1 (log phase). Cells were spun at 6000 g for 5 min at room temperature. Pellets were washed in Pi- and carbohydrate-deficient SC_u media. Cells were brought to OD_{600} ~0.025–0.03 in low-Pi (25 μM) SC_u media containing 0.5% sucrose with freshly made 2.0% galactose, and growth was monitored at 30 °C in an orbital shaker through log phase. After about 30 h of growth in low-Pi containing media, yeast cells were collected for RNA extraction as described (Collart & Oliviero 2001). Prior to cDNA synthesis, 0.3–0.5 μg of RNA was DNase-treated with RNase-free RQ DNase (Promega, Madison, WI, USA). cDNA was synthesized using the Superscript III First-Strand Synthesis System for RT-PCR (Invitrogen, Carlsbad, CA, USA). RT-PCR reactions of 30 cycles were performed using Ex-Taq polymerase (Takara Bio, Kyoto, Japan). ScActin was used as a reference gene. RT-PCR gene-specific primers are listed in Supporting Information Table S1. Qualitative analysis was determined via EtBr DNA gel and the ChemiDoc™ XRS+ System with Image Lab™ Software (Bio-Rad, Hercules, CA, USA). Adobe Photoshop CS3 software (San Jose, CA, USA) was used to organize images.

Subcellular localization

Plasmids expressing AtPht1;1 and AtPht1;1 Tyr 312 mutants in pEarleyGate101, TAIR stock #CD3-683 (Earley *et al*. 2006; Karimi *et al*. 2007) were used to transform *Agrobacterium tumefaciens* strain GV3101 by electroporation. *Nicotiana benthamiana* plants were grown in soil under long-day conditions at 23 °C for 4 weeks prior to transformation. AtPht1;1 and AtPht1;1^{Y312X} mutants were co-infiltrated with *A. tumefaciens* p19::pKYLX7 and PHF1::pCAMBIA-bar (Voinnet *et al*. 2003; Gonzalez *et al*. 2005; Brkljacic *et al*. 2009). *A. tumefaciens* cultures were grown to OD_{600} ~1.0 at 28 °C in an orbital shaker. The combination ratio of p19, PHF1, and each AtPht1;1 cDNA was 0.5:1.5:1.0, respectively. Cultures were combined and spun for 10 min at 2000 g. Pellets were washed with 1 mL of 10 mM $MgCl_2$ to remove antibiotics and resuspended in 2 mL of a resuspension solution (10 mM MES pH 5.9, 10 mM $MgCl_2$, 15 μM acetosyringone). Leaves were infiltrated immediately with 1 mL of the suspension. Plants were grown for 2–3 d after infiltration under the same conditions. Leaves were infiltrated with 50 μM FM4-64 (Setareh Biotech, Eugene, OR, USA) in water immediately preceding microscopy (Liesche *et al*. 2010; Lin *et al*. 2013). Imaging was captured at 40× using a Leica DM RXA2 deconvolution upright microscopy system in the Socolofsky Microscopy Center (Louisiana State University). Adobe Photoshop software was used to organize images.

^{32}P uptake assays

Cells were prepared as previously described for yeast complementation assays in SC_u media (25 μM Pi, 0.5% sucrose, 2.0% galactose) and brought to OD_{600} ~0.05. Once in log phase, cells were collected by repeating washes as previously described (Pi- and carbohydrate-free SC_u media). Cells were brought to OD_{600} 4.0–12.0 with Pi-free SC_u media containing 3% glucose (Lau *et al*. 1998; Catarecha *et al*. 2007; Ai *et al*. 2009; Lundh *et al*. 2009). $K_2H^{32}PO_4/KH_2PO_4$ solutions were prepared using a final $K_2H^{32}PO_4$ concentration of 2.5 μM with the remaining addition of KH_2PO_4 to obtain total Pi concentrations of 2.5 μM and 10 μM. For total Pi concentrations of 50, 100 and 250 μM, $K_2H^{32}PO_4/KH_2PO_4$ solutions were prepared using a final $K_2H^{32}PO_4$ concentration of 25 μM with the remaining addition of KH_2PO_4. 500 μM, 750 μM, and 1000 μM Pi concentration were prepared using a final $K_2H^{32}PO_4$ concentration of 50 μM. Two hundred microlitres of cells were used per each $K_2H^{32}PO_4/KH_2PO_4$ solution for a total volume of 250 μL. $K_2H^{32}PO_4/KH_2PO_4$ solutions containing no cells were used for obtaining $K_2H^{32}PO_4$ background activity. Following the addition of $K_2H^{32}PO_4$, assays were terminated after 6 min by passing 100 μL of cells through separate filter-lined syringes (MCE Membrane Filter, 0.45 μM, TISCH Scientific, North Bend, OH, USA), filtering once with 10 mL ice-cold 100 mM KH_2PO_4, followed by two passes of air to dry filter (Wykoff & O'Shea 2001; Catarecha *et al*. 2007). Filters were placed in scintillation vials containing 4 mL ScintiVerse BD Cocktail (Fisher Scientific) for counting by a Beckman LS 6000IC.

Arabidopsis genome identifiers

Genes from the above work include At4g13510 (*AtAMT1;1*), At5g43350 (*AtPht1;1*) and At2g38940 (*AtPht1;4*).

RESULTS

AtPht1;1 and AtPht1;4 proteins interact

A SLC assay optimized for *Arabidopsis* protoplasts (Kato & Jones 2010) was used to determine the homomeric and heteromeric assembly capabilities of Pht1;1 and Pht1;4. This method has been used previously to identify interactions among *Arabidopsis* syntaxin proteins (Fujikawa & Kato 2007), as well as ammonium transporters (Lalonde *et al*. 2010). *Pht1;1* and *Pht1;4* cDNAs were cloned into plasmids

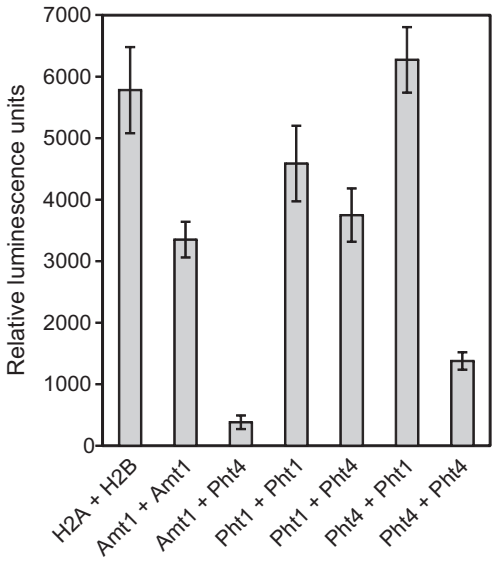

Figure 1. Pht1;1 and Pht1;4 interact to form homomeric and heteromeric oligomers. Amt1;1 (Amt1), Pht1;1 (Pht1), and/or Pht1;4 (Pht4) were co-expressed in *Arabidopsis* protoplasts for split luciferase complementation analysis. Amt1;1 homomeric interactions and Amt1;1 co-expressed with Pht1;4 served as positive and negative controls, respectively. Results were obtained from at least two independent experiments carried out in triplicate with evaluation of standard full-length Renilla luciferase activity and NLuc-H2A and H2B-CLuc interaction activities. Data are means ± SD.

containing the N-terminal (NLuc) and C-terminal (CLuc) halves of *Renilla* luciferase, in which the C-terminal end of each cDNA was fused to the corresponding fragment. As positive controls, we also examined the homomeric interaction of the *Arabidopsis* AMT1;1 ammonium transporter (Ludewig *et al*. 2003; Lalonde *et al*. 2010) and H2A and H2B heteromeric interactions (Fujikawa & Kato 2007). As shown in Fig. 1, luciferase activity was observed for homomeric Pht1;1 and heteromeric Pht1;1-Pht1;4 at levels comparable with the AMT1;1 and H2A–H2B controls. The luciferase activity for homomeric Pht1;4 was lower, but was still above that for the AMT1;1-Pht1;4 negative control. Together the data indicate oligomerization capabilities of Pht1;1 and Pht1;4 *in vivo*. *In vitro* analysis using co-immunoprecipitation confirmed the interactions between Pht1;1 and Pht1;4 (Fig. 2). Polyclonal antibodies were raised against Pht1;4 and Pht1;1/Pht1;2/Pht1;3 (because of the high sequence identity among Pht1;1, Pht1;2, and Pht1;3, and thus the unlikelihood of generating Pht1;1-specific antibodies, a peptide identical among these three Pht1 proteins was used to raise the antibodies). Pht1;1/2/3 and Pht1;4 were immunoprecipitated from total microsomal proteins isolated from root tissue of wild type or the *pht1;4* mutant (Misson *et al*. 2004) using anti-Pht1;1/2/3 and anti-Pht1;4 antibodies, respectively. Subsequent immunoblot analysis of bound proteins was performed with the corresponding antibody to confirm homomeric and heteromeric interactions. As a negative control, total microsomal proteins were immunoprecipitated without the addition of antibodies, resulting in no detection of unbound IP products. The analysis of bound Pht1;4 from *pht1;4* fractions served as an additional negative control and resulted in a lack of Pht1;4 signal.

The mating-based split-ubiquitin system (mbSUS) has been adapted to observe interactions of PM-bound proteins (Obrdlik *et al*. 2004; Grefen *et al*. 2007, 2009; Chen *et al*. 2012). We used the mbSUS system to further validate interactions between Pht1;1 and Pht1;4. Ubiquitin specific proteases recognize the formation of a full-length ubiquitin protein as a result of interacting proteins. These enzymes allow for the activation of the lexA promoter-driven reporter genes *LacZ*, *ADE2* and *HIS3* (Grefen *et al*. 2009). *AMT1;1*, *Pht1;1* and *Pht1;4* cDNAs were cloned into vectors containing the C-terminal half of ubiquitin (X-CUb) fused to the C-terminal end of the target protein and/or the N-terminal mutated half of ubiquitin (NUbG-X) fused to the N-terminus of proteins. The I13G mutation of the N-terminal half of ubiquitin prevents spontaneous reconstitution of ubiquitin (Grefen *et al*. 2009). Plasmids were mobilized into appropriate *Saccharomyces cerevisiae* haploid *a* and α strains and mated. Interactions were measured by observing growth on selective media (SC_{ahtlum}) with 10 mM 3-aminotriazole

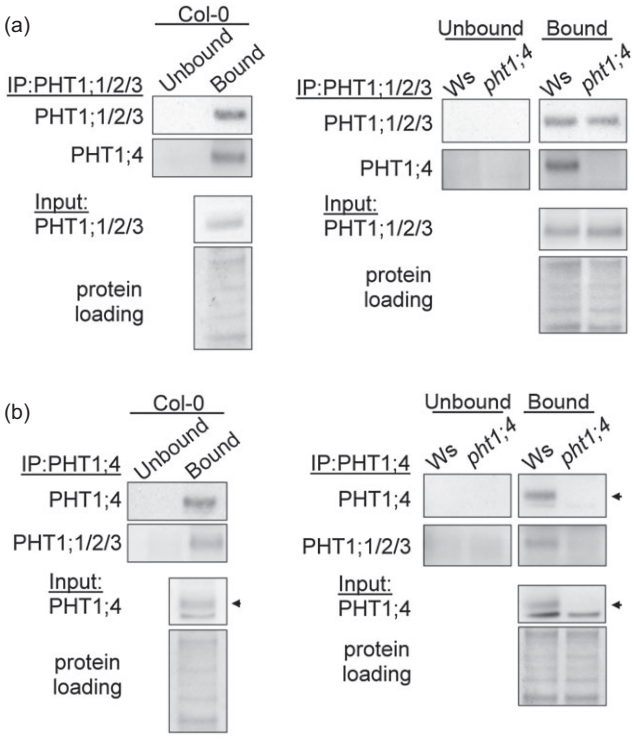

Figure 2. Pht1 immunoprecipitation (IP) of root microsomal proteins. Microsomal proteins were isolated from roots of Col-0 and Ws wild type and *pht1;4* mutants. Native Pht1;1/2/3 (a) or Pht1;4 (b) and their interacting proteins were immunoprecipitated by specific antibodies. IP products were loaded for detecting Pht1;1/2/3 or Pht1;4 by immunoblot (bound). IP without adding antibodies was used as a negative control (unbound). The levels of Pht1;1/2/3 (a) or Pht1;4 (b) in root microsomal protein fractions are shown in the lower panels.

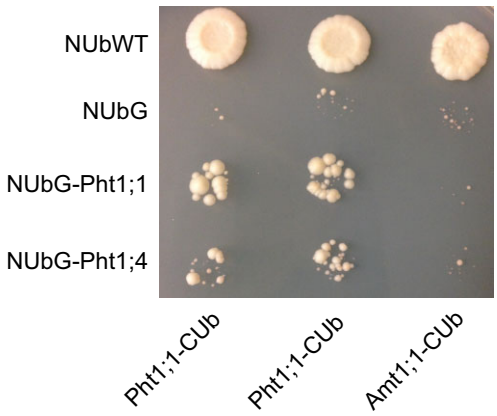

Figure 3. Split-ubiquitin assays in yeast confirm homomeric and heteromeric interactions of Pht1;1 and Pht1;4. Positive split-ubiquitin interactions were identified on minimal media (SC_{ahtlum}) containing 10 mM 3-aminotriazole. As a positive control, growth was monitored for matings of each of Amt1;1, Pht1;1, and Pht1;4 with the non-mutated amino fragment of ubiquitin, NUbWT. Amt1;1, Pht1;1, and Pht1;4 mating with NUbG, the mutated N-terminal half of ubiquitin, as well as Amt1;1 mating with Pht1;1 and Pht1;4 served as negative controls.

(3-AT), which was shown in preliminary experiments to remove false positives (data not shown), as in previous studies (Zhang *et al.* 2009). For controls, AMT1;1-CUb, Pht1;1-CUb and Pht1;4-CUb were mated with NUbWT (NUbI), the native N-terminal half of ubiquitin, and NUbG, the mutated N-terminal half of ubiquitin, lacking a target protein. As shown in Fig. 3, growth was observed for matings between cells expressing ubiquitin fragment fusions of Pht1;1 and Pht1;4, but not for the negative control matings between AMT1;1 and Pht1;1 or Pht1;4. Split-ubiquitin yeast-two-hybrid analysis further confirmed the interaction of Pht1;4 with itself and Pht1;1 by monitoring β-galactosidase activity (Supporting Information Fig. S1).

The role of a conserved protein motif in Pht1 oligomerization

Prior to the availability of the three-dimensional structure of PiPT, a Pi transporter from the endophytic fungus *P. indica* (Pedersen *et al.* 2013), we generated a putative Pht1;1 homomeric structure using Phyre2 Fold Recognition and Chimera software to identify potential protein interfaces based on molecular and biochemical similarities of known oligomeric crystal structures (Pettersen *et al.* 2004; Kelley & Sternberg 2009). Pht1;1 monomeric (Supporting Information Fig. S2a) and dimeric (Supporting Information Fig. S3) models were created by superimposing Pht1;1 to the structure of *Escherichia coli* multidrug transporter EmrD [RCSB Protein Data Bank (PDB) entry 2GFP], an MFS protein that produced high confidence scores with the Pht1;1 alignment, suggestive of overall protein fold overlap (91% coverage; 99.95% confidence; 13% identity) (Yin *et al.* 2006). From the dimeric model and sequence similarity among Pi transporters from plants and yeast, we identified a highly conserved motif, WFLLDIAFY (Supporting Information Fig. S4), in the seventh transmembrane alpha helix, which occupied the potential interface between monomers of a hypothetical Pht1;1 dimer (Supporting Information Fig. S3).

Upon release of the PiPT structure (PDB 4J05), a new model of Pht1;1 was generated using the Phyre2 server (Supporting Information Fig. S2b). Interestingly, PiPT was the second highest scoring template and the structure of *E. coli* XylE, a GLUT1-4 homolog (PDB 4GBZ), was the highest scoring, most likely because the large intracellular loop between helix 6 and 7 (residues 230–298) is not present in the PiPT structure, possibly because of this region being disordered. The structure of XylE was also released after the initial model of Pht1;1 was made. The new model of Pht1;1 is based on both the PiPT and XylE structures with >90% confidence in the model for 96% of the sequence (Supporting Information Fig. S2b). Whether PiPT functions as an oligomer has not been investigated. Trimeric arrangements of PiPT monomers in the same orientation were observed within crystals used to determine the PiPT structure (Pedersen *et al.* 2013). Although it is not clear how likely this trimer reflects a physiological structure, we aligned our second Pht1;1 model (based on XylE and PiPT; Supporting Information Fig. S2b) with the putative PiPT trimer (Supporting Information Fig. S5). The WFLLDIAFY conserved motif within helix 7 is within the pore and makes contacts with helices 9, 10 and 12, which form the putative trimer interface. Even though GLUT1-4 is known to oligomerize, the crystal structure of XylE did not reveal quaternary structure.

To determine the role of the WFLLDIAFY motif in interaction, we made several mutations (W304R, F305E, D308A, I309E, F311E and Y312D) simultaneously to generate Pht1;1-m, and also generated Pht1;1 proteins containing each individual mutated residue. All mutants were each co-expressed with native Pht1;1 in protoplasts and interaction was measured using SLC (Fig. 4). Protoplasts expressing Pht1;1 and either $Pht1;1^{F305E}$, $Pht1;1^{D308A}$, $Pht1;1^{I309E}$ or $Pht1;1^{F311E}$ resulted in reconstituted luciferase activity corresponding to 54.4–102.9% of the luciferase activity of the homomeric Pht1;1 interaction. The high relative luminescence (281.3%) observed for the interaction between Pht1;1 and $Pht1;1^{W304R}$ remains unclear, but will be studied further in the future. In contrast, we observed a significant lack of luciferase activity with native Pht1;1 co-expressed with Pht1;1-m, which may be attributed to the Y312D mutation (Fig. 4; see later).

Tyr 312 plays a role in AtPht1;1 interaction and function

We found that when Pht1;1 was mutated to $Pht1;1^{Y312D}$, interaction of the Pht1;1 homo-oligomer was disrupted (Fig. 4). RT-PCR of RNA extracted from co-transformed protoplasts confirmed that lack of luminescence in the SLC experiments was not due to a defect in $Pht1;1^{Y312D}$ expression (Supporting Information Fig. S6). To better understand the role of Tyr 312 in homomeric Pht1;1 interaction, we generated two addi-

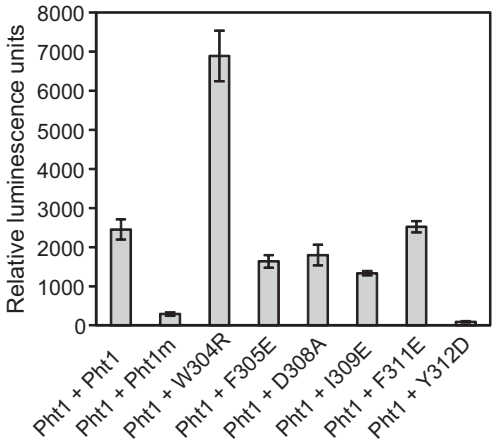

Figure 4. Interaction of the Pht1;1 homo-oligomer is abolished by mutation of Tyr 312. The native Pht1;1 sequence fused to the amino fragment of luciferase (NLuc) was co-expressed with native Pht1;1, a Pht1;1 variant containing six site-directed mutations (mut), or individual site-directed mutants (as indicated) in *Arabidopsis* protoplasts for split luciferase complementation analysis. Results were obtained from two independent experiments carried out in triplicate with standard full-length *Renilla* luciferase activity and NLuc-H2A and H2B-CLuc interaction activity. Data are means ± SD.

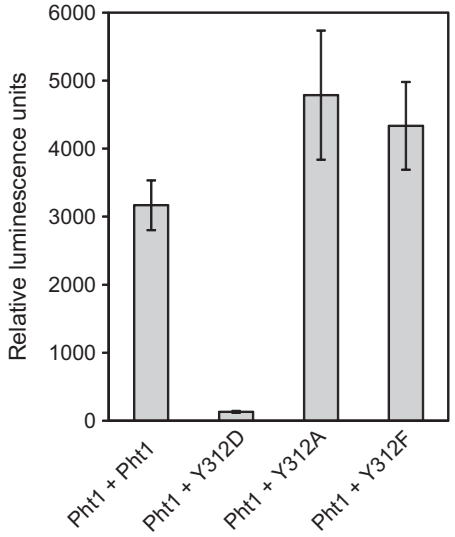

Figure 5. Pht1;1 homomeric interaction is abolished by the Y312D mutation, but not by Y312A or Y312F. Pht1;1 (Pht1) was co-expressed with itself or a site-directed mutant (as indicated) in *Arabidopsis* protoplasts for split luciferase complementation analysis. Results were obtained from two independent experiments with standard full-length Renilla luciferase activity and NLuc-H2A and H2B-CLuc interaction activity. Data are means ± S.D.

tional mutants, Pht1;1^{Y312A} and Pht1;1^{Y312F}. We found reconstituted luciferase activity for the interaction between native Pht1;1 and each mutant at a level similar to the homomeric native Pht1;1 interaction (Fig. 5). Thus, mutation of Tyr 312 to Asp, but not Ala or Phe, abolishes Pht1;1 homo-oligomerization. To determine whether changes in interaction were associated with improper processing (e.g. localization) of Pht1;1^{Y312D}, we transiently expressed YFP fusions of the Tyr 312 mutants in *N. benthamiana* leaves. Because infiltration of Pht1;1 and Tyr 312 mutants alone resulted in little visual detection (data not shown), co-infiltration was performed with p19, an RNAi silencing suppressor previously used to enhance fluorescence *in planta* (Baulcombe & Molnar 2004; Brkljacic *et al*. 2009) and AtPHF1 (Gonzalez *et al*. 2005; Bayle *et al*. 2011). Prior to microscopy, the PM of epidermal cells was stained with FM4-64, an endocytic marker (Liesche *et al*. 2010; Bayle *et al*. 2011; Lin *et al*. 2013). As shown in Fig. 6, we observed co-localization of FM4-64 and each of the Pht1;1^{Y312D}, Pht1;1^{Y312A} and Pht1;1^{Y312F} proteins, indicating that mutations of Tyr 312 did not disrupt the localization of Pht1;1.

Heterologous expression of plant Pht1 proteins in Pi-uptake defective yeast strains has been used previously to characterize Pi transporter activities (Bun-ya *et al*. 1996; Yompakdee *et al*. 1996; Leggewie *et al*. 1997; Smith *et al*. 1997; Liu *et al*. 2008, 2014a; Jia *et al*. 2011). Herein we used this system to determine the impact of the Tyr 312 mutations on Pht1;1 activity. The mutant *S. cerevisiae* yeast strain PAM2 (Δpho89::*TRP1* Δpho84::*HIS3 ade2 leu2 his3 trp1 ura3*) was transformed with pYES2 plasmids containing Pht1;1, Pht1;1^{Y312D}, Pht1;1^{Y312A} or Pht1;1^{Y312F} under the control of a galactose-inducible promoter. For controls, PAM2 was transformed with the native yeast Pht1 Pi transporter, ScPho84, or empty vector. RT-PCR experiments confirmed comparable transgene expression in the yeast isolates (Supporting Information Fig. S7). Yeast cells were grown on Pi-sufficient media, washed with Pi-free media, and inoculated into media containing galactose and a low level of Pi (25 μM). Cell growth (OD at Ab_{600}) was monitored, and growth rate coefficients were determined (Supporting Information Fig. S8). Several independently obtained growth rate coefficients ($n \geq 3$) and corresponding doubling times were calculated for each cell type (Fig. 7, Supporting Information Table S2). As expected, cells expressing Pho84 exhibited a higher growth rate than cells containing the empty pYES2 vector, consistent with Pho84-complementation of the PAM2 Pi-uptake defect. Expression of Pht1;1, Pht1;1^{Y312A}, or Pht1;1^{Y312F} also complemented this defect, but only moderately. These results suggest that the Y312A and Y312F mutations did not affect Pht1;1 function. In contrast, the growth rate of cells expressing Pht1;1^{Y312D} exceeded that of Pht1;1 by 1.5-fold, a level comparable with that of Pho84-complemented cells, suggesting enhanced Pi transport activity of Pht1;1 by the Y312D mutation.

To determine whether the increased growth rate of yeast expressing Pht1;1^{Y312D} was due to enhanced Pi uptake capabilities, we performed ^{32}P uptake assays to compare the kinetic properties of Pht1;1 and Pht1;1^{Y312D}. Yeast cells were grown in Pi-replete media to log phase, washed with Pi-free media, and subjected to short-term ^{32}Pi uptake assays with varying external Pi concentrations. Representative assays for cells expressing Pht1;1 or Pht1;1^{Y312D} are shown in Supporting Information Fig. S9. Both cell lines showed Michaelis–Menten kinetics and exhibited similar K_m values of 544 μM

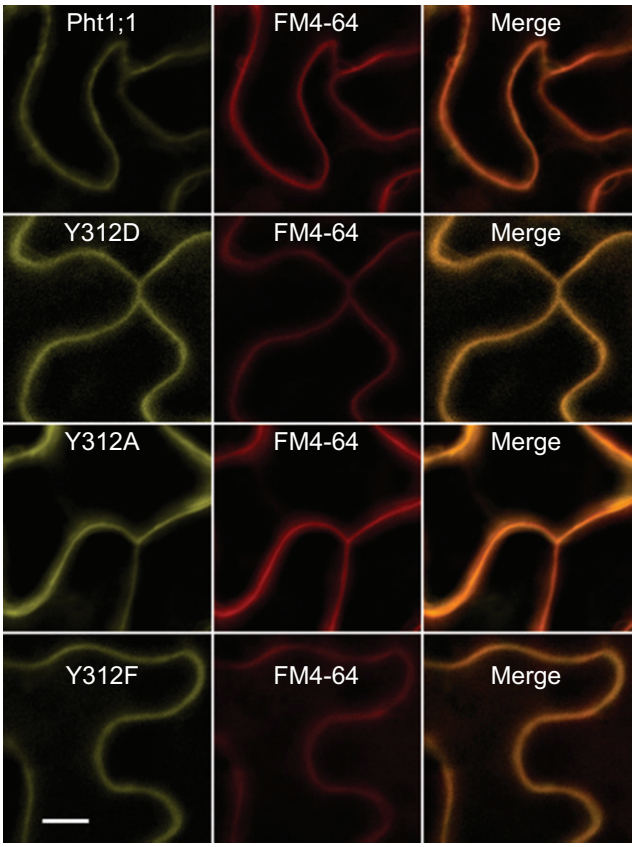

Figure 6. Intracellular plasma membrane localization of Pht1;1 is not disrupted by mutation of Tyr 312. *Nicotiana benthamiana* leaves of 4-week-old plants were transiently transformed by agro-infiltration with Pht1;1, Pht1;1^{Y312D}, Pht1;1^{Y312A}, or Pht1;1^{Y312F} and co-infiltrated with p19, a gene-silencing suppressor, and PHF1, a Pht1 facilitator protein. Leaves were infiltrated with the endocytic marker FM4-64 prior to deconvolution microscopy. Merged images of Pht1;1 and Tyr 312 mutants with FM4-64 show overlapping localization of YFP and red fluorescence. Size bar = 10 μm.

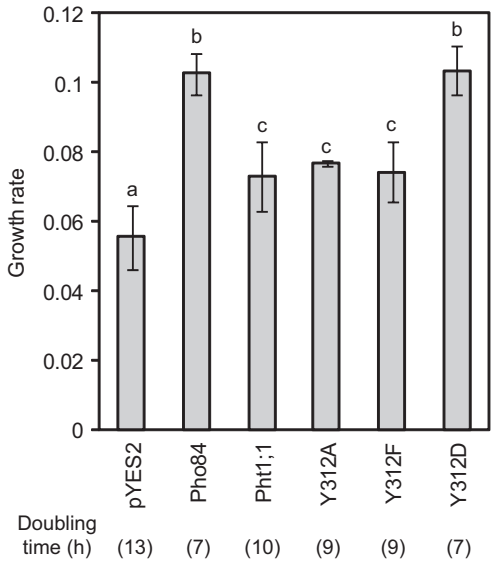

Figure 7. The Y312D mutation of Pht1;1 confers enhanced growth to Pi-uptake defective PAM2 yeast cells when grown under low-Pi conditions. The mutant *Sacharomyces cerevisiae* yeast strain PAM2 was complemented with Gal1 promoter-driven pYES2 plasmids containing Pht1;1, Pht1;1^{Y312D}, Pht1;1^{Y312A}, or Pht1;1^{Y312F}. PAM2 cells were transformed with native yeast high-affinity phosphate transporter Pho84 or an empty vector for positive and negative controls, respectively. Transformants were grown in SC_u media containing 25 μM phosphate with 0.5% sucrose and 2.0% galactose, and growth rate was monitored for up to 48 h. Growth coefficients were derived using exponential regression analysis during logarithmic growth ($n \geq 3$). Data are means ± SD.

Table 1. Kinetic properties of Pht1;1 and Pht1;1^{Y312D}

Genotype	K_m μM	V_{max} pmol 10^7 cells^{-1} min^{-1}
PAM2 + pYES2:Pht1;1	544 ± 95	101 ± 8
PAM2 + pYES2:Pht1;1^{Y312D}	581 ± 74	707 ± 47

Pht1;1 and *Pht1;1^{Y312D}* cDNAs were expressed in the PAM2 yeast mutant using pYES2. Representative transformants expressing each cDNA were used in ^{32}P uptake assays, measured for nine phosphate concentrations between 0 and 1000 μM for 6 min. The kinetic constants were calculated from Michaelis–Menten plots generated via non-linear regression in KaleidaGraph for results obtained from three independent experiments run in duplicate and are the mean ± SD ($n = 3$).

and 581 μM, respectively (Table 1), indicating that Y312D does not affect the Pi affinity of Pht1;1. In contrast, the V_{max} for Pht1;1^{Y312D} was sevenfold higher relative to Pht1;1 (Table 1), suggesting that the Y312D mutation enhances the Pi uptake capacity of Pht1;1.

DISCUSSION

Oligomerization of Pht1 proteins was implied by observations in some earlier studies, but was not implicitly demonstrated (Chiou *et al*. 2001; Catarecha *et al*. 2007; Nussaume *et al*. 2011). Herein we used *in vivo* and *in vitro* interaction assays to directly show that Pht1;1 and Pht1;4 form homomeric and heteromeric oligomers. Upon observing interaction among Pht1 monomers we sought to investigate the nature of the oligomeric unit. Visual examination of high molecular weight bands on Pht1 immunoblots from previous studies (Chiou *et al*. 2001; Nussaume *et al*. 2011) indicated the presence of possible dimers and tetramers. With this information and by searching known protein structures in the RCSB PDB for those sharing similarity to Pht1;1, we generated three-dimensional models of Pht1;1 using EmrD as a template (Supporting Information Fig. S2a) and later using XylE and PiPT (Supporting Information Fig. S2b). EmrD, XylE and PiPT are MFS proteins with standard topology of 12 transmembrane helices (Yin *et al*. 2006). Structural determination of EmrD revealed two identical molecules present as a dimer in the asymmetric unit of the crystal lattice; although whether this packing arrangement is physiological is unclear (Yin *et al*. 2006). Using EmrD as a template, we

generated a dimeric model of Pht1;1 and identified the amino acids present in the putative interaction region, WFLLDIAFY, which corresponded to transmembrane helix 7 (Supporting Information Fig. S3). Unlike EmrD, PiPT orients helix 7 towards the centre of the transporter pore, where three amino acids in helix 7, W320, D324 and Y328, are reported to play an important role in Pi binding (Pedersen *et al*. 2013). Ironically, our data show that mutagenesis of this conserved Tyr (Y312 in Pht1;1) to Asp interferes with oligomerization (Fig. 4). As PiPT presumably serves as a better model for Pht1;1 than EmrD because of higher sequence identity and a shared biological function, it is likely that helix 7 of Pht1;1 occupies the central portion of the cylinder where several of its residues occupy the Pi-binding site, rather than occupying a putative interaction region between two hypothetical Pht1;1 monomers. The asymmetric unit within PiPT crystals used to determine its structure contains trimeric arrangements of PiPT monomers in the same orientation (Pedersen *et al*. 2013). The interface of this trimer involves interactions between helices 9, 10 and 12, which also border the WFLLDIAFY motif in helix 7. Based on the dynamic nature of MFS proteins during transport, it is possible that activity is linked to oligomerization through allosteric events coupling helix 7 with the interface. Mutations in the active site, like Tyr 312 to an Asp, may be translated to the surface favouring the monomeric or oligomeric state. Additional studies are required to ascertain the oligomeric composition of Pht1 proteins.

The heterologous expression of Pht1 transporters in yeast has previously demonstrated a wide range of kinetic parameters for individual Pht1 proteins (Leggewie *et al*. 1997; Daram *et al*. 1998; Rausch *et al*. 2004; Liu *et al*. 2008, 2014a; Ai *et al*. 2009; Jia *et al*. 2011). Indeed, despite overlapping tissue-specific expression patterns, including the root epidermis, and their presumed high-affinity activities, the Pht1 proteins LePT1, StPT2, MtPT1 and MtPT2 were shown to have K_m values of 31, 130, 587 and 641 μM (Leggewie *et al*. 1997; Daram *et al*. 1998; Liu *et al*. 2008). *MtPT1* and *MtPT2* share relatively high sequence identity with *Pht1;1*, and all three genes contain 5′-UTR introns (Liu *et al*. 2008). Although determining orthology is complicated by differential expansion of Pht1 gene families in individual plant species (Liu *et al*. 2008), the similarities among MtPT1, MtPT2 and Pht1;1 suggest they are functionally equivalent. Our finding that the K_m of Pht1;1 (544 μM) is very similar to those of MtPT1 (587 μM) and MtPT2 (641 μM) further support this notion.

In addition to affecting oligomerization, our data indicate that the Y312D mutation enhances Pi transport of Pht1;1 in yeast. We found that Pht1;1 partially complemented the PAM2 mutant, whereas Pht1;1^{Y312D} complemented the mutant as well as the native yeast Pho84 transporter (Fig. 7). This is likely due to the sevenfold increase in V_{max} for Pht1;1^{Y312D} relative to Pht1;1, as shown by short-term ^{32}Pi uptake analysis (Table 1). These uptake experiments also suggest that Pht1;1 and Pht1;1^{Y312D} exhibit similar Pi affinities, with K_m values of 544 μM and 581 μM, respectively (Table 1). V_{max} is a function of the enzyme concentration, in this case the abundance of transporter at the PM, and the catalysis rate (k_{cat}), in this case the release of Pi from the transporter into the cytosol. K_m is also a function of k_{cat}, as well as two additional terms: k_f, the binding of Pi to the transporter, and k_r, the extracellular release of Pi. As k_{cat} is shared by both V_{max} and K_m, and a change in k_{cat} would thus affect both parameters, it is possible that the concentration of functional transporters differs between Pht1;1 and Pht1;1^{Y312D}. RT-PCR experiments showed the transgenes were expressed at comparable levels, suggesting an equivalent number of transporter monomers, although the Y312D mutation might alter post-translational regulatory mechanisms, such as PM targeting or degradation/recycling of Pht1 (Bayle *et al*. 2011). However, our observations from the transient localization of Pht1;1 and Pht1;1^{Y312D} in *N. benthamiana* leaves (Fig. 6) implies that the Y312D mutation does not have a major effect on PM localization. Pht1;1 as an oligomer may restrict its Pi transport capacity relative to Pht1;1^{Y312D} by allowing only a portion of the oligomer to be receptive to Pi binding at any given time. This would be similar to the MFS lactose transporter, LacS, which, like Pht1 transporters, operates via a 'rocker-switch' mechanism where only the intracellular or extracellular side of the transporter is open. LacS functions as a dimer, and the orientation of one monomer (i.e. outside-facing or inside-facing) is coupled to the opposite orientation in the other monomer (Veenhoff *et al*. 2001). Another explanation for Pht1;1 and Pht1;1^{Y312D} having the same K_m, but a different V_{max} is that substitution of Tyr 312 with Asp creates a more favourable environment that reduces extracellular release of Pi (k_r) and enhances intracellular release of Pi (k_{cat}). Based on the PiPT structure, the conserved Tyr (Y328 in PiPT) is predicted to occupy the Pi-binding site of the transporter where it, along with five additional conserved residues, coordinates Pi (Pedersen *et al*. 2013). Among the five additional residues is an Asp (D308 in Pht1;1), whose alternating protonation/deprotonation plays a key role in the movement of Pi through the transporter. It is possible that replacing Tyr 312 with an Asp still allows for Pi binding (i.e. does not affect K_f), but provides additional negative charge upon deprotonation that results in a faster release of Pi through the transporter (i.e. lower k_r and/or higher k_{cat}).

Environmental conditions, such as Pi availability, could induce Pht1;1 interactions as a means of Pi-uptake regulation, similar to the situation for *Arabidopsis* nitrate transporter NRT1.1. Previously, NRT1.1 was identified as having two distinct uptake affinities, that is low affinity and high affinity, under the control of a 'phosphorylation switch' (Liu *et al*. 1999; Liu & Tsay 2003; Ho *et al*. 2009; Gutierrez 2012; Parker & Newstead 2014). Structural analysis revealed that phosphorylation decouples NRT1.1 homomeric interactions, leading to the reorganization of functional monomers with high-affinity nitrate uptake capabilities (Sun *et al*. 2014). Pht1 transporters too have been shown to undergo modifications in response to environmental conditions to maintain Pi homeostasis (Bayle *et al*. 2011; Huang *et al*. 2013; Lin *et al*. 2013). Under Pi-replete conditions, Pht1;1 transporter accumulation is controlled by various transcriptional and post-translational regulatory mechanisms and includes the recycling and/or degradation of Pht1;1 transporters at the

PM in the presence of excess Pi (Bayle *et al*. 2011; Huang *et al*. 2013; Lin *et al*. 2013). While oligomerization does not appear to alter the Pi affinity of Pht1 transporters, a mechanism comparable with the oligomeric function of NRT1.1 could occur with Pht1;1 as an immediate form of regulation prior to the down-regulation, retention and degradation of Pht1 transporters as described by the regulatory roles of NLA, PHO2 and PHF1 (Bayle *et al*. 2011; Huang *et al*. 2013; Lin *et al*. 2013). This may correlate with the temporal and spatial differences recently described between the PHO2- and NLA-mediated pathways despite their abilities to function cooperatively in the degradation of Pht1;1 and Pht1;4 upon Pi-replete conditions (Huang *et al*. 2013; Lin *et al*. 2013).

AMTs were previously shown to form phosphorylation-dependent oligomers as a means of providing transporter regulation for rapid transport inactivation to prevent ammonium over-accumulation (Loque *et al*. 2007; Lanquar *et al*. 2009; Yuan *et al*. 2013). Also, the Amt1;1 trimeric complex is proposed to regulate ammonium transport via a gate mechanism (Loque *et al*. 2007, 2009). Oligomeric forms of Pht1 could act in a regulatory mechanism similar to AMTs to inactivate or down-regulate Pi uptake. If the trimeric form of PiPT represented in Pedersen *et al*. (2013) has biological significance, this may suggest a higher-order structure for Pht1;1 similar to that of Amt1;1. Alternatively, interactions between Pi transporter monomers may modify the position of transmembrane helices to control substrate access and/or transport through the pore. This perception may be relevant to interlaced models of Pht1;1 based on structures of EmrD and PiPT, where perhaps the monomeric state positions Tyr 312 within the pore to engage in Pi binding/transport, whereas the oligomeric state may energetically favour Tyr 312 (i.e. helix 7) to shift along the periphery of the protein to trigger interaction and close pore access (Forrest *et al*. 2011). Future experiments aimed at deciphering the relative impact of the Y312D mutation on transporter activity and oligomerization under fluctuating Pi conditions should shed additional light on these open questions.

ACKNOWLEDGMENTS

We would like to thank Wayne Versaw for providing the *N. benthamiana* seeds and the p19 construct. We also thank David Donze, John Larkin, Grover Waldrop and Marcia Newcomer for insightful discussions.

DISCLOSURES

No conflicts of interest declared.

FINANCIAL SOURCES

This work was supported by the National Science Foundation Plant Genome Research Program (IOS-1127051 to A.P.S.), the National Science Foundation Graduate Research Fellowship Program (DGE-1247192 to E.B.F.) and a grant from the Academia Sinica of Taiwan (AS-103-TP-B11 to T.-J.C.).

AUTHOR CONTRIBUTIONS

A.P.S. and E.B.F. designed the research, performed experiments, analysed data and wrote the paper. S.F.D., N.K., T.J.C., M.A.M., D.M.O., R.D. and W.Y.L. performed experiments and analysed data.

REFERENCES

Ai P., Sun S., Zhao J., Fan X., Xin W., Guo Q., . . . Xu G. (2009) Two rice phosphate transporters, OsPht1;2 and OsPht1;6, have different functions and kinetic properties in uptake and translocation. *Plant Journal* **57,** 798–809.

Aung K., Lin S.I., Wu C.C., Huang Y.T., Su C.L. & Chiou T.J. (2006) pho2, a phosphate overaccumulator, is caused by a nonsense mutation in a microRNA399 target gene. *Plant Physiology* **141,** 1000–1011.

Bari R., Datt Pant B., Stitt M. & Scheible W.R. (2006) PHO2, microRNA399, and PHR1 define a phosphate-signaling pathway in plants. *Plant Physiology* **141,** 988–999.

Baulcombe D.C. & Molnar A. (2004) Crystal structure of p19 – a universal suppressor of RNA silencing. *Trends in Biochemical Sciences* **29,** 279–281.

Bayle V., Arrighi J.F., Creff A., Nespoulous C., Vialaret J., Rossignol M., . . . Nussaume L. (2011) *Arabidopsis thaliana* high-affinity phosphate transporters exhibit multiple levels of posttranslational regulation. *The Plant Cell* **23,** 1523–1535.

Brkljacic J., Zhao Q. & Meier I. (2009) WPP-domain proteins mimic the activity of the HSC70-1 chaperone in preventing mistargeting of RanGAP1-anchoring protein WIT1. *Plant Physiology* **151,** 142–154.

Bun-ya M., Shikata K., Nakade S., Yompakdee C., Harashima S. & Oshima Y. (1996) Two new genes, PHO86 and PHO87, involved in inorganic phosphate uptake in *Saccharomyces cerevisiae*. *Current Genetics* **29,** 344–351.

Catarecha P., Segura M.D., Franco-Zorrilla J.M., Garcia-Ponce B., Lanza M., Solano R., . . . Leyva A. (2007) A mutant of the *Arabidopsis* phosphate transporter PHT1;1 displays enhanced arsenic accumulation. *The Plant Cell* **19,** 1123–1133.

Chen J., Lalonde S., Obrdlik P., Noorani Vatani A., Parsa S.A., Vilarino C., . . . Rhee S.Y. (2012) Uncovering *Arabidopsis* membrane protein interactome enriched in transporters using mating-based split ubiquitin assays and classification models. *Front Plant Sciences* **3,** 124.

Chiou T.J., Liu H. & Harrison M.J. (2001) The spatial expression patterns of a phosphate transporter (MtPT1) from *Medicago truncatula* indicate a role in phosphate transport at the root/soil interface. *The Plant Journal: For Cell and Molecular Biology* **25,** 281–293.

Clarke O.B. & Gulbis J.M. (2012) Oligomerization at the membrane: potassium channel structure and function. *Advances in Experimental Medicine and Biology* **747,** 122–136.

Collart M.A. & Oliviero S. (2001) Preparation of yeast RNA. *Current Protocols Molecular Biology* **13,** Unit 13.12.

Daram P., Brunner S., Persson B.L., Amrhein N. & Bucher M. (1998) Functional analysis and cell-specific expression of a phosphate transporter from tomato. *Planta* **206,** 225–233.

Daram P., Brunner S., Rausch C., Steiner C., Amrhein N. & Bucher M. (1999) Pht2;1 encodes a low-affinity phosphate transporter from *Arabidopsis*. *The Plant Cell* **11,** 2153–2166.

Devaiah B.N., Karthikeyan A.S. & Raghothama K.G. (2007) WRKY75 transcription factor is a modulator of phosphate acquisition and root development in *Arabidopsis*. *Plant Physiology* **143,** 1789–1801.

Duby G., Hosy E., Fizames C., Alcon C., Costa A., Sentenac H. & Thibaud J.B. (2008) AtKC1, a conditionally targeted Shaker-type subunit, regulates the activity of plant K+ channels. *The Plant Journal: For Cell and Molecular Biology* **53,** 115–123.

Duttweiler H.M. (1996) A highly sensitive and non-lethal beta-galactosidase plate assay for yeast. *Trends in Genetics* **12,** 340–341.

Earley K.W., Haag J.R., Pontes O., Opper K., Juehne T., Song K. & Pikaard C.S. (2006) Gateway-compatible vectors for plant functional genomics and proteomics. *The Plant Journal: For Cell and Molecular Biology* **45,** 616–629.

Fan C., Wang X., Hu R., Wang Y., Xiao C., Jiang Y., . . . Fu Y.F. (2013) The pattern of Phosphate transporter 1 genes evolutionary divergence in Glycine max L. *BMC Plant Biology* **13,** 48.

Forrest L.R., Kramer R. & Ziegler C. (2011) The structural basis of secondary active transport mechanisms. *Biochimica et Biophysica Acta* **1807,** 167–188.

Fujikawa Y. & Kato N. (2007) Split luciferase complementation assay to study protein-protein interactions in *Arabidopsis* protoplasts. *The Plant Journal: For Cell and Molecular Biology* **52,** 185–195.

Geitz K.A., Richter D.W. & Gottschalk A. (1995) The influence of chemical and mechanical feedback on ventilatory pattern in a model of the central respiratory pattern generator. *Advances in Experimental Medicine and Biology* **393,** 23–28.

Gonzalez E., Solano R., Rubio V., Leyva A. & Paz-Ares J. (2005) PHOSPHATE TRANSPORTER TRAFFIC FACILITATOR1 is a plant-specific SEC12-related protein that enables the endoplasmic reticulum exit of a high-affinity phosphate transporter in *Arabidopsis*. *The Plant Cell* **17,** 3500–3512.

Graff L., Obrdlik P., Yuan L., Loque D., Frommer W.B. & von Wiren N. (2011) N-terminal cysteines affect oligomer stability of the allosterically regulated ammonium transporter LeAMT1;1. *Journal of Experimental Botany* **62,** 1361–1373.

Grefen C., Lalonde S. & Obrdlik P. (2007) Split-ubiquitin system for identifying protein-protein interactions in membrane and full-length proteins. *Current Protocols Neuroscience* **5,** Unit 5.27.

Grefen C., Obrdlik P. & Harter K. (2009) The determination of protein-protein interactions by the mating-based split-ubiquitin system (mbSUS). *Methods in Molecular Biology* **479,** 217–233.

Gutierrez R.A. (2012) Systems biology for enhanced plant nitrogen nutrition. *Science* **336,** 1673–1675.

Ho C.H., Lin S.H., Hu H.C. & Tsay Y.F. (2009) CHL1 functions as a nitrate sensor in plants. *Cell* **138,** 1184–1194.

Ho S.N., Hunt H.D., Horton R.M., Pullen J.K. & Pease L.R. (1989) Site-directed mutagenesis by overlap extension using the polymerase chain reaction. *Gene* **77,** 51–59.

Huang T.K., Han C.L., Lin S.I., Chen Y.J., Tsai Y.C., Chen Y.R., . . . Chiou T.J. (2013) Identification of downstream components of ubiquitin-conjugating enzyme PHOSPHATE2 by quantitative membrane proteomics in *Arabidopsis* roots. *The Plant Cell* **25,** 4044–4060.

Jia H., Ren H., Gu M., Zhao J., Sun S., Zhang X., . . . Xu G. (2011) The phosphate transporter gene OsPht1;8 is involved in phosphate homeostasis in rice. *Plant Physiology* **156,** 1164–1175.

Kant S., Peng M. & Rothstein S.J. (2011) Genetic regulation by NLA and microRNA827 for maintaining nitrate-dependent phosphate homeostasis in *Arabidopsis*. *PLoS Genetics* **7,** e1002021.

Karimi M., Depicker A. & Hilson P. (2007) Recombinational cloning with plant gateway vectors. *Plant Physiology* **145,** 1144–1154.

Kataoka T., Watanabe-Takahashi A., Hayashi N., Ohnishi M., Mimura T., Buchner P., . . . Takahashi H. (2004) Vacuolar sulfate transporters are essential determinants controlling internal distribution of sulfate in *Arabidopsis*. *The Plant Cell* **16,** 2693–2704.

Kato N. & Jones J. (2010) The split luciferase complementation assay. *Methods in Molecular Biology* **655,** 359–376.

Kelley L.A. & Sternberg M.J. (2009) Protein structure prediction on the Web: a case study using the Phyre server. *Nature Protocols* **4,** 363–371.

Lalonde S., Sero A., Pratelli R., Pilot G., Chen J., Sardi M.I., . . . Frommer W.B. (2010) A membrane protein/signaling protein interaction network for *Arabidopsis* version AMPv2. *Front Physiology* **1,** 24.

Lanquar V., Loque D., Hormann F., Yuan L., Bohner A., Engelsberger W.R., . . . Frommer W.B. (2009) Feedback inhibition of ammonium uptake by a phospho-dependent allosteric mechanism in *Arabidopsis*. *The Plant Cell* **21,** 3610–3622.

Lau W.W., Schneider K.R. & O'Shea E.K. (1998) A genetic study of signaling processes for repression of PHO5 transcription in *Saccharomyces cerevisiae*. *Genetics* **150,** 1349–1359.

LeBlanc M.S., McKinney E.C., Meagher R.B. & Smith A.P. (2013) Hijacking membrane transporters for arsenic phytoextraction. *Journal of Biotechnology* **163,** 1–9.

Leggewie G., Willmitzer L. & Riesmeier J.W. (1997) Two cDNAs from potato are able to complement a phosphate uptake-deficient yeast mutant: identification of phosphate transporters from higher plants. *The Plant Cell* **9,** 381–392.

Liesche J., He H.X., Grimm B., Schulz A. & Kuhn C. (2010) Recycling of *Solanum* sucrose transporters expressed in yeast, tobacco, and in mature phloem sieve elements. *Molecular Plant* **3,** 1064–1074.

Lin W.Y., Huang T.K. & Chiou T.J. (2013) Nitrogen limitation adaptation, a target of microRNA827, mediates degradation of plasma membrane-localized phosphate transporters to maintain phosphate homeostasis in *Arabidopsis*. *The Plant Cell* **25,** 4061–4074.

Liu J., Versaw W.K., Pumplin N., Gomez S.K., Blaylock L.A. & Harrison M.J. (2008) Closely related members of the *Medicago truncatula* PHT1 phosphate transporter gene family encode phosphate transporters with distinct biochemical activities. *The Journal of Biological Chemistry* **283,** 24673–24681.

Liu K.H. & Tsay Y.F. (2003) Switching between the two action modes of the dual-affinity nitrate transporter CHL1 by phosphorylation. *The EMBO Journal* **22,** 1005–1013.

Liu K.H., Huang C.Y. & Tsay Y.F. (1999) CHL1 is a dual-affinity nitrate transporter of *Arabidopsis* involved in multiple phases of nitrate uptake. *The Plant Cell* **11,** 865–874.

Liu P., Chen S., Song A., Zhao S., Fang W., Guan Z., . . . Chen F. (2014a) A putative high affinity phosphate transporter, CmPT1, enhances tolerance to Pi deficiency of chrysanthemum. *BMC Plant Biology* **14,** 18.

Liu T.Y., Lin W.Y., Huang T.K. & Chiou T.J. (2014b) MicroRNA-mediated surveillance of phosphate transporters on the move. *Trends in Plant Science* **19,** 647–655.

Loque D., Lalonde S., Looger L.L., von Wiren N. & Frommer W.B. (2007) A cytosolic trans-activation domain essential for ammonium uptake. *Nature* **446,** 195–198.

Loque D., Mora S.I., Andrade S.L., Pantoja O. & Frommer W.B. (2009) Pore mutations in ammonium transporter AMT1 with increased electrogenic ammonium transport activity. *The Journal of Biological Chemistry* **284,** 24988–24995.

Ludewig U., Wilken S., Wu B., Jost W., Obrdlik P., El Bakkoury M., . . . Frommer W.B. (2003) Homo- and hetero-oligomerization of ammonium transporter-1 NH4 uniporters. *The Journal of Biological Chemistry* **278,** 45603–45610.

Lundh F., Mouillon J.M., Samyn D., Stadler K., Popova Y., Lagerstedt J.O., . . . Persson B.L. (2009) Molecular mechanisms controlling phosphate-induced downregulation of the yeast Pho84 phosphate transporter. *Biochemistry* **48,** 4497–4505.

Marianayagam N.J., Sunde M. & Matthews J.M. (2004) The power of two: protein dimerization in biology. *Trends in Biochemical Sciences* **29,** 618–625.

Matthews J.M. & Sunde M. (2012) Dimers, oligomers, everywhere. *Advances in Experimental Medicine and Biology* **747,** 1–18.

Misson J., Thibaud M.C., Bechtold N., Raghothama K. & Nussaume L. (2004) Transcriptional regulation and functional properties of *Arabidopsis* Pht1;4, a high affinity transporter contributing greatly to phosphate uptake in phosphate deprived plants. *Plant Molecular Biology* **55,** 727–741.

Muchhal U.S., Pardo J.M. & Raghothama K.G. (1996) Phosphate transporters from the higher plant *Arabidopsis thaliana*. *Proceedings of the National Academy of Sciences of the United States of America* **93,** 10519–10523.

Mudge S.R., Rae A.L., Diatloff E. & Smith F.W. (2002) Expression analysis suggests novel roles for members of the Pht1 family of phosphate transporters in *Arabidopsis*. *The Plant Journal: For Cell and Molecular Biology* **31,** 341–353.

Nagarajan V.K., Jain A., Poling M.D., Lewis A.J., Raghothama K.G. & Smith A.P. (2011) *Arabidopsis* Pht1;5 mobilizes phosphate between source and sink organs and influences the interaction between phosphate homeostasis and ethylene signaling. *Plant Physiology* **156,** 1149–1163.

Nussaume L., Kanno S., Javot H., Marin E., Pochon N., Ayadi A., . . . Thibaud M.C. (2011) Phosphate import in plants: focus on the PHT1 transporters. *Front Plant Sciences* **2,** 83.

Obrdlik P., El-Bakkoury M., Hamacher T., Cappellaro C., Vilarino C., Fleischer C., . . . Frommer W.B. (2004) K+ channel interactions detected by a genetic system optimized for systematic studies of membrane protein interactions. *Proceedings of the National Academy of Sciences of the United States of America* **101,** 12242–12247.

Okamoto M., Kumar A., Li W., Wang Y., Siddiqi M.Y., Crawford N.M. & Glass A.D. (2006) High-affinity nitrate transport in roots of *Arabidopsis* depends on expression of the NAR2-like gene AtNRT3.1. *Plant Physiology* **140,** 1036–1046.

Orsel M., Chopin F., Leleu O., Smith S.J., Krapp A., Daniel-Vedele F. & Miller A.J. (2006) Characterization of a two-component high-affinity nitrate uptake system in *Arabidopsis*. Physiology and protein–protein interaction. *Plant Physiology* **142,** 1304–1317.

Pao S.S., Paulsen I.T. & Saier M.H. Jr. (1998) Major facilitator superfamily. *Microbiology and Molecular Biology Reviews* **62,** 1–34.

Park B.S., Seo J.S. & Chua N.H. (2014) NITROGEN LIMITATION ADAPTATION recruits PHOSPHATE2 to target the phosphate transporter PT2 for degradation during the regulation of *Arabidopsis* phosphate homeostasis. *The Plant Cell* **26,** 454–464.

Parker J.L. & Newstead S. (2014) Molecular basis of nitrate uptake by the plant nitrate transporter NRT1.1. *Nature* **507,** 68–72.
Pedersen B.P., Kumar H., Waight A.B., Risenmay A.J., Roe-Zurz Z., Chau B.H., . . . Stroud R.M. (2013) Crystal structure of a eukaryotic phosphate transporter. *Nature* **496,** 533–536.
Pettersen E.F., Goddard T.D., Huang C.C., Couch G.S., Greenblatt D.M., Meng E.C. & Ferrin T.E. (2004) UCSF chimera – a visualization system for exploratory research and analysis. *Journal of Computational Chemistry* **25,** 1605–1612.
Raghothama K.G. (2000) Phosphate transport and signaling. *Current Opinion in Plant Biology* **3,** 182–187.
Rausch C., Zimmermann P., Amrhein N. & Bucher M. (2004) Expression analysis suggests novel roles for the plastidic phosphate transporter Pht2;1 in auto- and heterotrophic tissues in potato and *Arabidopsis*. *The Plant Journal: For Cell and Molecular Biology* **39,** 13–28.
Reddy V.S., Shlykov M.A., Castillo R., Sun E.I. & Saier M.H. Jr. (2012) The major facilitator superfamily (MFS) revisited. *The FEBS Journal* **279,** 2022–2035.
Reinders A., Schulze W., Kuhn C., Barker L., Schulz A., Ward J.M. & Frommer W.B. (2002a) Protein–protein interactions between sucrose transporters of different affinities colocalized in the same enucleate sieve element. *The Plant Cell* **14,** 1567–1577.
Reinders A., Schulze W., Thaminy S., Stagljar I., Frommer W.B. & Ward J.M. (2002b) Intra- and intermolecular interactions in sucrose transporters at the plasma membrane detected by the split-ubiquitin system and functional assays. *Structure (London, England: 1993)* **10,** 763–772.
Remy E., Cabrito T.R., Batista R.A., Teixeira M.C., Sa-Correia I. & Duque P. (2012) The Pht1;9 and Pht1;8 transporters mediate inorganic phosphate acquisition by the *Arabidopsis thaliana* root during phosphorus starvation. *The New Phytologist* **195,** 356–371.
Rojas-Triana M., Bustos R., Espinosa-Ruiz A., Prat S., Paz-Ares J. & Rubio V. (2013) Roles of ubiquitination in the control of phosphate starvation responses in plants. *Journal of Integrative Plant Physiology* **55,** 40–53.
Rouached H., Wirtz M., Alary R., Hell R., Arpat A.B., Davidian J.C., . . . Berthomieu P. (2008) Differential regulation of the expression of two high-affinity sulfate transporters, SULTR1.1 and SULTR1.2, in *Arabidopsis*. *Plant Physiology* **147,** 897–911.
Schulze W.X., Reinders A., Ward J., Lalonde S. & Frommer W.B. (2003) Interactions between co-expressed *Arabidopsis* sucrose transporters in the split-ubiquitin system. *BMC Biochemistry* **4,** 3.
Shin H., Shin H.S., Dewbre G.R. & Harrison M.J. (2004) Phosphate transport in *Arabidopsis*: Pht1;1 and Pht1;4 play a major role in phosphate acquisition from both low- and high-phosphate environments. *The Plant Journal: For Cell and Molecular Biology* **39,** 629–642.
Smith F.W., Ealing P.M., Dong B. & Delhaize E. (1997) The cloning of two *Arabidopsis* genes belonging to a phosphate transporter family. *The Plant Journal: For Cell and Molecular Biology* **11,** 83–92.
Sun J., Bankston J.R., Payandeh J., Hinds T.R., Zagotta W.N. & Zheng N. (2014) Crystal structure of the plant dual-affinity nitrate transporter NRT1.1. *Nature* **507,** 73–77.
Veenhoff L.M., Heuberger E.H.M.L. & Poolman B. (2001) The lactose transport protein is a cooperative dimer with two sugar translocation pathways. *The EMBO Journal* **20,** 3056–3062.
Voinnet O., Rivas S., Mestre P. & Baulcombe D. (2003) An enhanced transient expression system in plants based on suppression of gene silencing by the p19 protein of tomato bushy stunt virus. *The Plant Journal: For Cell and Molecular Biology* **33,** 949–956.
Wang H., Xu Q., Kong Y.H., Chen Y., Duan J.Y., Wu W.H. & Chen Y.F. (2014) *Arabidopsis* WRKY45 transcription factor activates PHOSPHATE TRANSPORTER1;1 expression in response to phosphate starvation. *Plant Physiology* **164,** 2020–2029.
Wirth J., Chopin F., Santoni V., Viennois G., Tillard P., Krapp A., . . . Gojon A. (2007) Regulation of root nitrate uptake at the NRT2.1 protein level in *Arabidopsis thaliana*. *The Journal of Biological Chemistry* **282,** 23541–23552.
Wykoff D.D. & O'Shea E.K. (2001) Phosphate transport and sensing in *Saccharomyces cerevisiae*. *Genetics* **159,** 1491–1499.
Yin Y., He X., Szewczyk P., Nguyen T. & Chang G. (2006) Structure of the multidrug transporter EmrD from *Escherichia coli*. *Science* **312,** 741–744.
Yompakdee C., Ogawa N., Harashima S. & Oshima Y. (1996) A putative membrane protein, Pho88p, involved in inorganic phosphate transport in *Saccharomyces cerevisiae*. *Molecular and General Genetics* **251,** 580–590.
Yuan L., Gu R., Xuan Y., Smith-Valle E., Loque D., Frommer W.B. & von Wiren N. (2013) Allosteric regulation of transport activity by heterotrimerization of *Arabidopsis* ammonium transporter complexes *in vivo*. *The Plant Cell* **25,** 974–984.
Zhang L.Y., Bai M.Y., Wu J., Zhu J.Y., Wang H., Zhang Z., . . . Wang Z.Y. (2009) Antagonistic HLH/bHLH transcription factors mediate brassinosteroid regulation of cell elongation and plant development in rice and *Arabidopsis*. *The Plant Cell* **21,** 3767–3780.

Received 21 November 2014; received in revised form 6 February 2015; accepted for publication 14 February 2015

SUPPORTING INFORMATION

Additional Supporting Information may be found in the online version of this article at the publisher's web-site:

Figure S1. Pht1;1 and Pht1;4 interactions observed using the split-ubiquitin Y2H system.
Figure S2. A model of Pht1;1 based on the structure of (a) EmrD and (b) PiPT and XylE.
Figure S3. A homodimer model of Pht1;1 based on the structure of EmrD.
Figure S4. A conserved motif among Pht1 proteins implicated in interaction.
Figure S5. A homotrimer model of Pht1;1 based on the structures of PiPT and XylE.
Figure S6. RT-PCR of RNA extracted from co-transformed protoplast preparations used for split luciferase complementation assays.
Figure S7. RT-PCR of RNA isolated from yeast shows similar transgene transcript abundance.
Figure S8. Representative growth assays of PAM2 yeast cells expressing empty pYES2 vector, Pho84, Pht1;1 or Pht1;1 Tyr 312 variants.
Figure S9. Representative ^{32}P uptake assays of PAM2 yeast cells expressing Pht1;1 or Pht1;1^{Y312D} via the pYES2 vector.
Table S1. PCR and RT-PCR primer sequences.
Table S2. Growth parameters for yeast cells expressing an empty pYES2 vector, or complemented with Pho84, Pht1;1, Pht1;1^{Y312A}, Pht1;1^{Y312F}, or Pht1;1^{Y312D}.